Supporting Information

A Highly Sensitive and Selective Near-Infrared Fluorescent Probe for Detecting Peroxynitrite in Living Cells and *Drosophila* Brains

Wei Wang, Jian-Bin Deng, Long Jin and Bai-Ou Guan*

Guangdong Provincial Key Laboratory of Optical Fiber Sensing and Communication, Institute of Photonics Technology, Jinan University, Guangzhou 511443, China;
wangwei_0415@jnu.edu.cn (W.W.); dengjianbin@stu2020.jnu.edu.cn (J.-B.D.);
tjinlong@jnu.edu.cn (L.J.)
* Correspondence: tguanbo@jnu.edu.cn; Tel: +86-20-37337012

Contents

1. Experimental Details

1.1. Reagents

1, 6-dihydroxynaphthalene was purchased from Shanghai Yien Chemical Technology Ltd. (Shanghai, China); methyl sulfonic acid and phthalic anhydride were purchased from Energy Chemical; *N*, *N*-dimethylformamide (DMF) and potassium carbonate were purchased from Aladdin; dimethyl sulfoxide (DMSO), manganese dioxide, ethylene diamine tetraacetic acid, and ferrous sulfate were purchased from Meryer; dipotassium hydrogen phosphate and potassium phosphate were purchased from Macklin; sodium nitrite was purchased from TCI; hydrogen peroxide (30%) was purchased from Guangzhou Guangtry Reagent Technology Ltd. (Guangzhou, China); glutathione (GSH), cysteine (Cys), homocysteine (Hcy), glucose (Glu), xanthine, 2-(4-(bromomethyl) phenyl)-4,4,5,5-tetramethyl-1,3,2-dioxaborolane, and sodium hypochlorite were purchased from Shanghai Bide Pharmaceutical Technology Co., Ltd. (Shanghai, China); xanthine oxidase and 3-(aminopropyl)-1-hydroxy-3-isopropyl-2-oxo-1-triazene (NOC-5) were purchased from Sigma-Aldrich (St. Louis, MO, USA); superoxide dismutase was purchased from Shanghai Yuanye Biotechnology Co., Ltd. (Shanghai, China); 3-morpholinosydnonimine hydrochloride (SIN-1) was purchased from Glpbio. All the solvents and reagents were commercial without further purification.

Peroxynitrite ($ONOO^-$) was prepared following the method reported in the literature [1]. In a nutshell, a mixture of sodium nitrite ($NaNO_2$, 0.6 M) and hydrogen peroxide (H_2O_2, 0.7 M) was acidified with hydrochloric acid (HCl, 0.6 M) and sodium hydroxide (NaOH, 1 M) was added right away to render the solution alkaline. Manganese dioxide was used to remove the hydrogen peroxide. The concentration of $ONOO^-$ was determined by UV analysis at 302 nm with an extinction coefficient of 1670 $M^{-1}cm^{-1}$. Aliquots of the solution were stored at −20 °C. $^{\bullet}OH$ was generated by the Fenton reaction ($Fe^{2+} + H_2O_2$), in which EDTA was used to avoid the precipitation of Fe^{2+} and Fe^{2+} concentration represented the $^{\bullet}OH$ concentrations [2]. NO was provided by donor 3-(aminopropyl)-1-hydroxy-3-isopropyl-2-oxo-1-triazene (NOC-5, 100 μM). $O_2^{\bullet-}$ was created by the enzymatic reaction of xanthine/xanthine oxidase (XA/XO; 6.0 μM/3 mU) at 25 °C for 5 min [3]. The $^1O_2$ was generated by reaction (100 μM H_2O_2 + 500 μM OCl^-). Other materials were used as received from commercial sources unless otherwise indicated. Ultrapure water was used throughout.

1.2. Apparatus

Absorption spectra were recorded with a UV–visible spectrophotometer (Techcomp, UV2310). Fluorescence measurements were measured on a spectrometer (Ocean Insight, QE Pro-Raman) with a 1 × 10 mm quartz cell at the slits of 5 nm, excited by a xenon lamp source (Zolix, Gloria-X150A). Images of the cells were taken on laser confocal microscope (Leica, SP8). Cell viability was tested by ELIASA (TECAN, SPARK 10M). Images of *Drosophila* brains were taken with a fluorescent stereomicroscope (Mshot, MZX81). ^1H NMR and ^{13}C NMR spectra were recorded on a Bruker 600MHZ spectrometer with $CDCl_3$ (TMS as internal standard) or DMSO-d_6. HRMS spectra were taken on a high-resolution mass spectrometer (Sciex, AB SCIEX 500R).

2. Synthesis Details and Characterizations

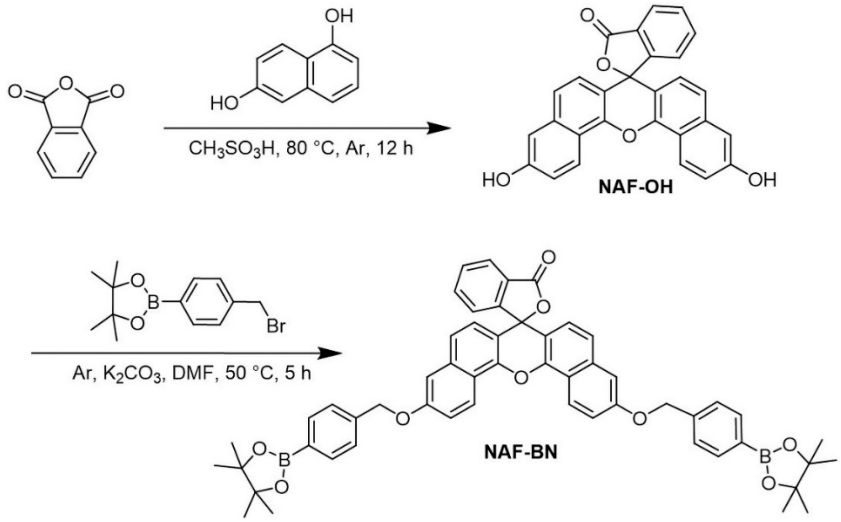

Scheme 1. Synthetic route of **NAF-OH** and **NAF-BN**.

2.1. Synthesis of NAF-OH

NAF-OH was synthesized according to the literature [4]. 1,6-dihydroxynaphthalene (6.25 g, 39 mmol) and phthalic anhydride (2.67 g, 18 mmol) were dissolved in 40 mL methane sulfonic acid stirred at 80 °C under argon. After 12 h, the reaction mixture was diluted with 400 mL ice-water and the crude product was obtained by decompression filtration. The crude material was purified by flash chromatography (ethyl acetate: petroleum ether = 1:1), a deep red solid was obtained (2.45 g, yield = 31%). ^{1}H NMR (600 MHz, DMSO–d_6) δ 10.17 (s, 2H), 8.68 (d, *J* = 9.0 Hz, 2H), 8.09 (d, *J* = 6.9 Hz, 1H), 7.84–7.68 (m, 2H), 7.45 (d, *J* = 8.7 Hz, 2H), 7.36 (dd, *J* = 9.0, 2.4 Hz, 2H), 7.30 (d, *J* = 6.8 Hz, 1H), 7.20 (d, *J* = 2.4 Hz, 2H), 6.70 (d, *J* = 8.7 Hz, 2H). ^{13}C NMR (151 MHz, DMSO–d_6) δ: 168.90, 157.38, 153.26, 146.08, 135.97, 135.84, 130.33, 125.81, 124.81, 124.24, 124.00, 123.82, 122.67, 119.34, 117.32, 109.46, 109.43, 83.27. HRMS (ESI): m/z, calculated for $C_{28}H_{17}O_5$, 433.1076 $[M+H]^+$, found: 433.1065.

2.2. Synthesis of NAF-BN

NAF-OH (100 mg, 0.234 mmol), K_2CO_3 (95.9 mg, 0.694 mmol), and 2-(4-(bromomethyl) phenyl)-4,4,5,5-tetramethyl-1,3,2-dioxaborolane (206 mg, 0.694 mmol) were dissolved in 5 mL dry DMF, stirred for 10 min, then reacted at 50 °C for 5 h. The mixture was then diluted with 30 mL ethyl acetate and washed with water and brine. The organic layer was dried with anhydrous sodium sulfate (Na_2SO_4) and filtered. The filtrate was concentrated under reduced pressure and purified by flash chromatography (ethyl acetate: petroleum ether = 1:2), a yellow solid was obtained (80 mg, yield = 40%). ^{1}H NMR (600 MHz, $CDCl_3$) δ 8.66 (d, *J* = 9.1 Hz, 2H), 8.13–8.05 (m, 1H), 7.86 (d, *J* = 7.5 Hz, 4H), 7.63 (d, *J* = 5.7, 3.0 Hz, 2H), 7.50 (d, *J* = 7.6 Hz, 4H), 7.45 (d, *J* = 9.1, 2.5 Hz, 2H), 7.37 (d, *J* = 8.6 Hz, 2H), 7.21 (d, *J* = 2.5 Hz, 2H), 7.16–7.08 (m, 1H), 6.80 (d, *J* = 8.7 Hz, 2H), 5.24 (s, 4H), 1.35 (s, 24H). ^{13}C NMR (151 MHz, $CDCl_3$) δ: 169.72, 158.29, 154.11, 146.73, 139.61, 135.94, 135.12, 135.04, 129.72, 126.63, 126.50, 126.05, 125.03, 124.63, 124.10, 123.86, 122.86, 119.40, 119.16, 110.67, 107.73, 83.86, 70.05, 65.30, 24.87. HRMS (ESI): m/z, calculated for $C_{53}H_{51}B_2O_9$, 865.3719 $[M+H]^+$, found: 865.3716.

3. Figures S1–S12

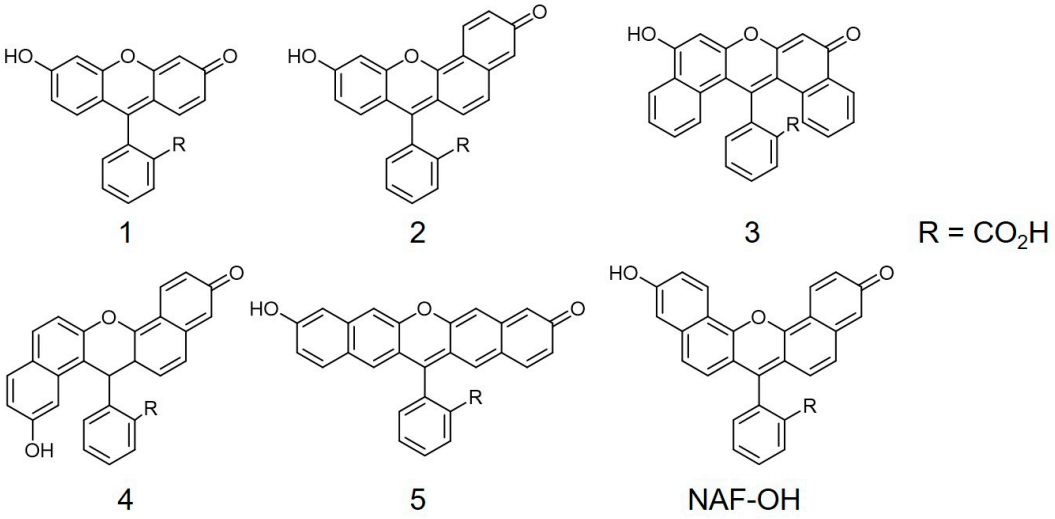

compound	$\lambda_{abs,\ max}$ (nm)	$\lambda_{em,\ max}$ (nm)	pK_a
1	491	513	6.33±0.04
2	538	629	7.76±0.04
3	534	565	6.02±0.04
4	610	674	>8
5	708	790	>8
NAF-OH	595	670	7.99±0.02

Figure S1. Structures and properties of naphthofluoresceins.

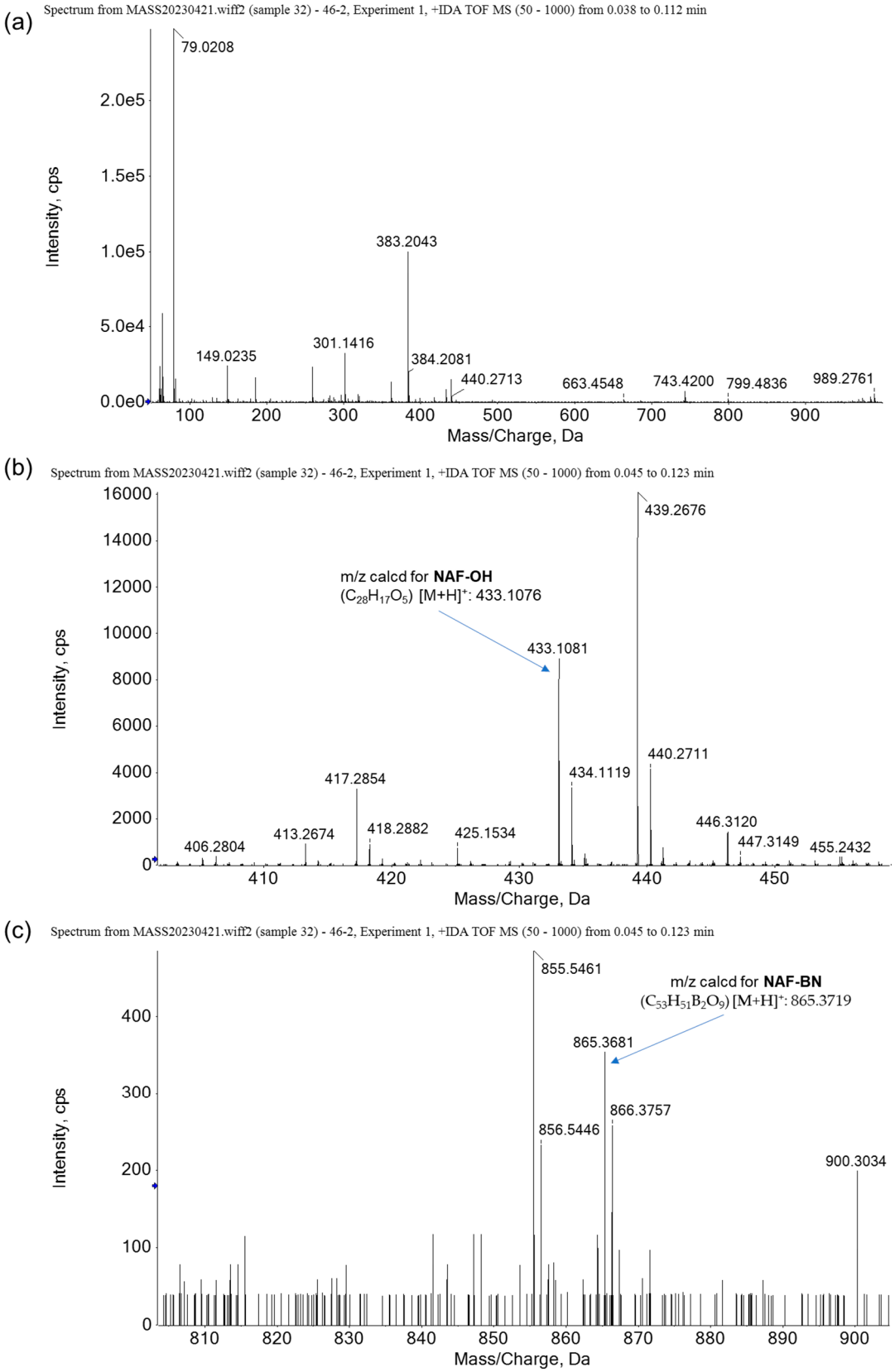

Figure S2. HRMS spectrum of **NAF-BN** (5 μM) after 15 min of reaction with $ONOO^-$ (100 μM), (**a**) full spectrum, (**b**) the spectrum of m/z = 400–460, (**c**) the spectrum of m/z = 810–900.

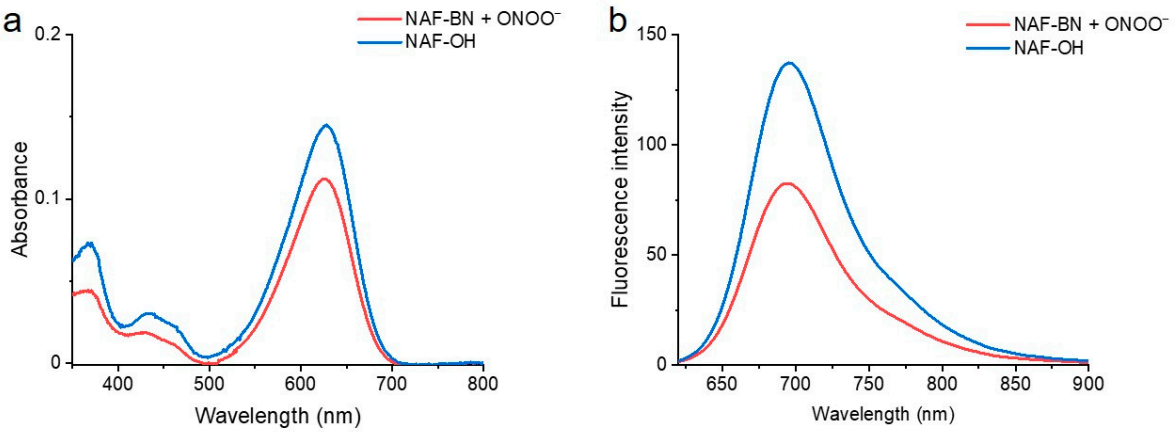

Figure S3. Absorption (**a**) and fluorescence spectra (**b**) of **NAF-OH** (blue line; 5 μM) and **NAF-BN** (5 μM) after reaction with $ONOO^-$ (100 μM) for 15 min (red line) in phosphate buffer (100 mM PB, pH 7.4, with 50% DMSO). λ_{ex} = 600 nm; slits = 5 nm/5 nm.

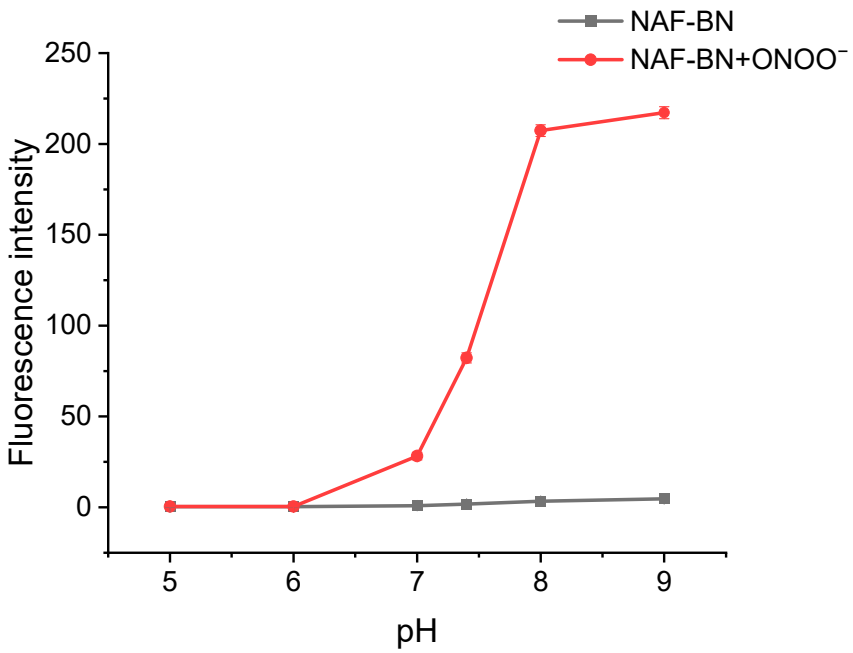

Figure S4. Effect of different pH values on the fluorescence of **NAF-BN** (5 μM) or **NAF-BN** (5 μM) with $ONOO^-$ (100 μM) after 1 h in phosphate buffer (100 mM PB, pH 7.4, with 50% DMSO). λ_{ex} = 600 nm, λ_{em} = 695 nm.

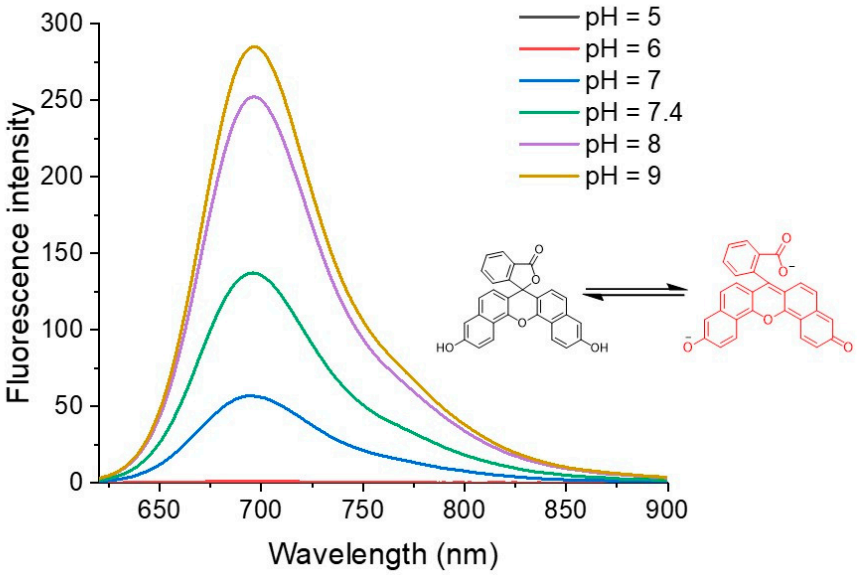

Figure S5. Fluorescence spectra of **NAF-OH** (5 μM) at different pH values, λ_{ex} = 600 nm, λ_{em} = 695 nm.

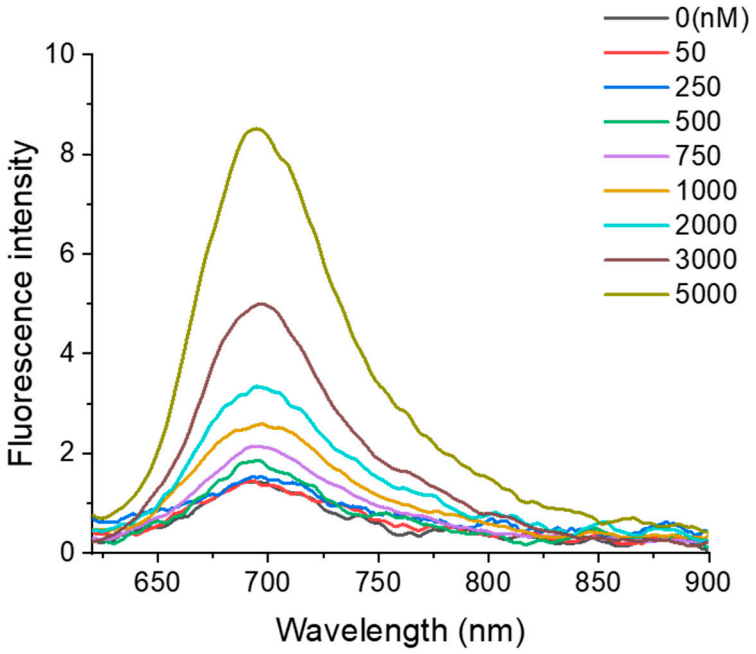

Figure S6. Fluorescence response to **NAF-BN** (5 μM) with different concentrations of $ONOO^-$ for 15 min, λ_{ex} = 600 nm, λ_{em} = 695 nm.

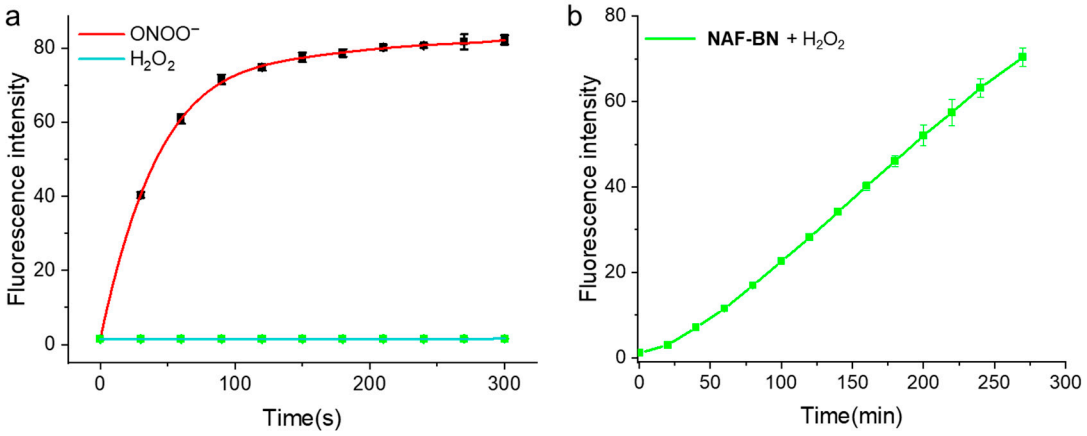

Figure S7. (**a**) Reaction of **NAF-BN** (5 μM) with $ONOO^-$ (100 μM) or H_2O_2 (100 μM); fluorescence intensity at 695 nm versus time (0–300 s). (**b**) Reaction of **NAF-BN** (5 μM) with H_2O_2 (100 μM); fluorescence intensity at 695 nm versus time (0–300 min). λ_{ex} = 600 nm, λ_{em} = 695 nm.

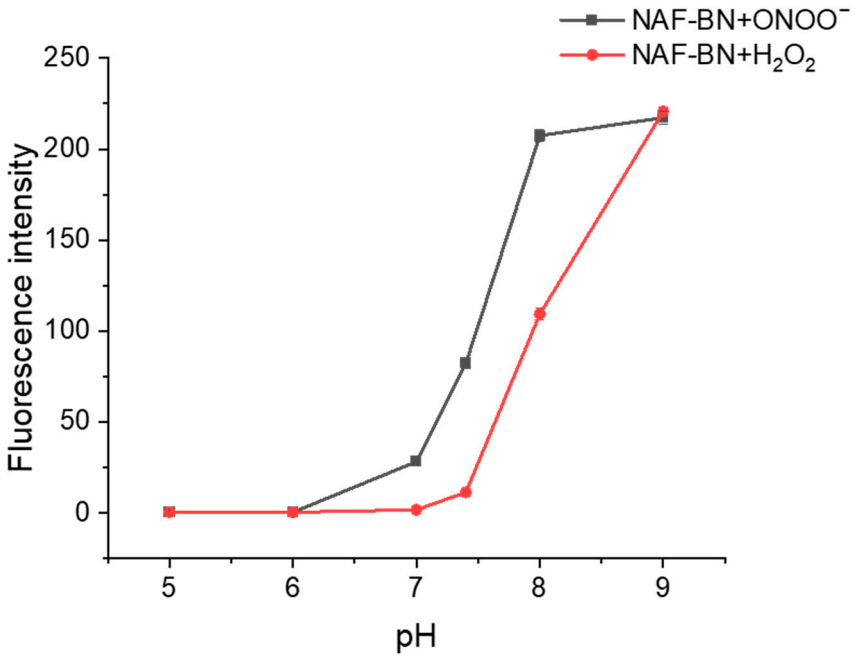

Figure S8. Effect of different pH values on the fluorescence of NAF-BN (5 μM) after reaction with $ONOO^-$ (100 μM) or H_2O_2 (100 μM) after 1 h in phosphate buffer (100 mM PB, pH 7.4, with 50% DMSO). λ_{ex} = 600 nm, λ_{em} = 695 nm.

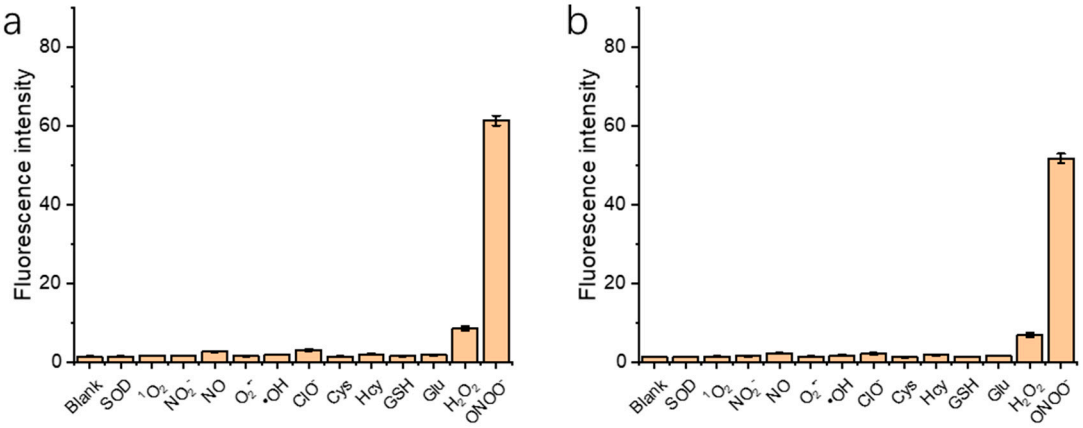

Figure S9. Fluorescence response to **NAF-BN** and different analytes for 15 min: ClO^-, $^1O_2$, NO_2^-, NO, $O_2^{\bullet-}$, •OH, Cys, Hcy, GSH, glucose, H_2O_2 (1 mM); $ONOO^-$ (100 μM); and SOD (50 U/mL). All experiments were performed in phosphate buffer (100 mM PB, pH 7.4, with 50% DMSO); the concentration of **NAF-BN** was 5 μM; λ_{ex} = 600 nm; slits = 5 nm/5 nm. (**a**) Acetonitrile/PB, 1/1, (**b**) 1,4-dioxane/PB, 1/1.

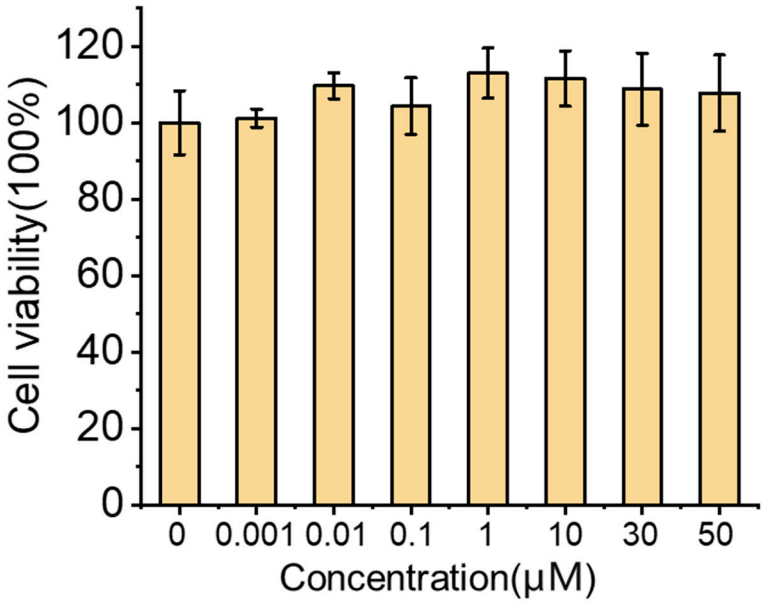

Figure S10. Cell viability of 4T1 cells incubated with different concentrations of **NAF-BN**, as assessed by CCK-8 assays (incubation time 24 h).

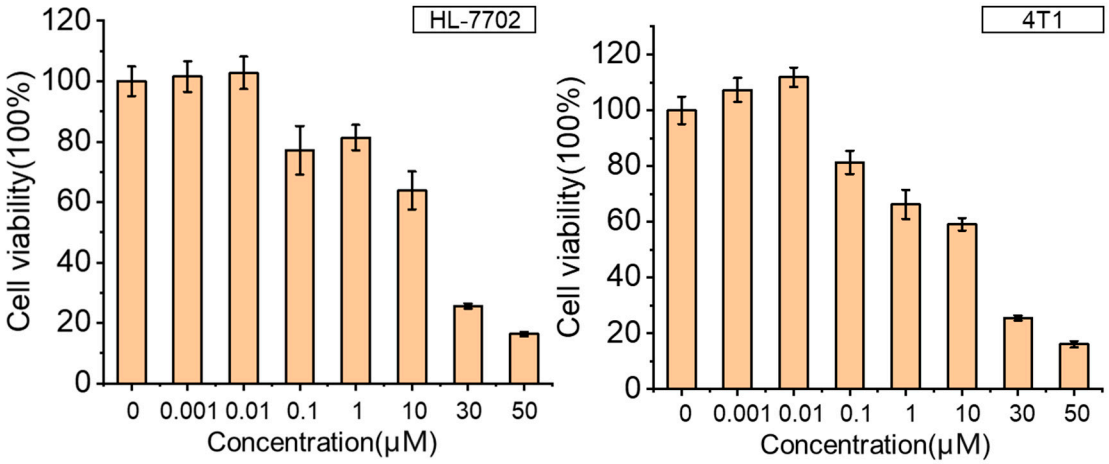

Figure S11. Cell viability of HL-7702 and 4T1 cells incubated with different concentrations of **NAF-OH**, as assessed by CCK-8 assays (incubation time 24 h).

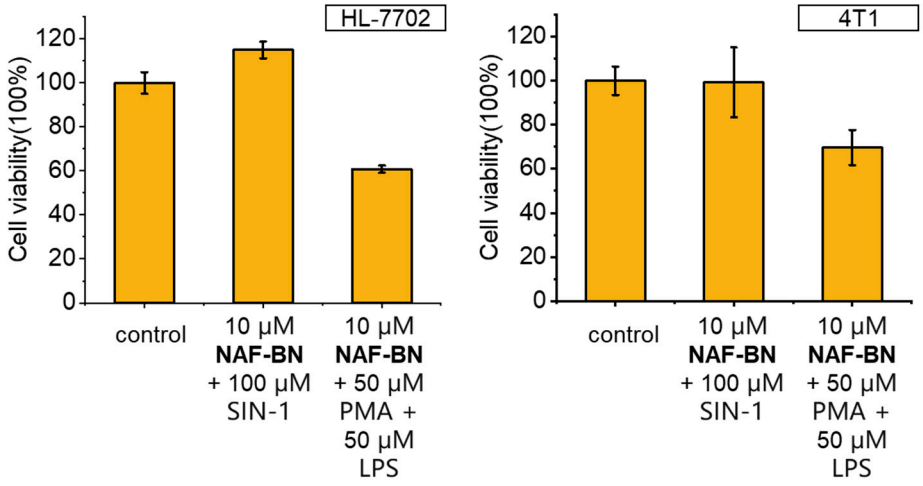

Figure S12. Cell viability of HL-7702 and 4T1 cells incubated with **NAF-BN** and SIN-1 or **NAF-BN** and PMA/LPS, as assessed by CCK-8 assays (incubation time 24 h).

4. NMR and HRMS Spectra

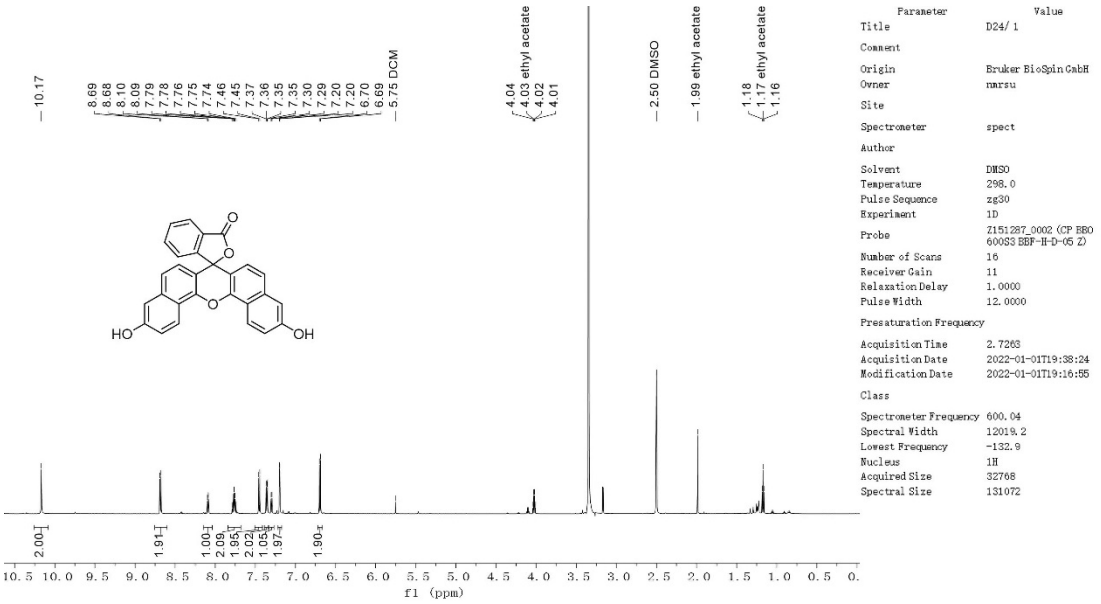

Figure S13. ^{1}H NMR spectrum of **NAF-OH**.

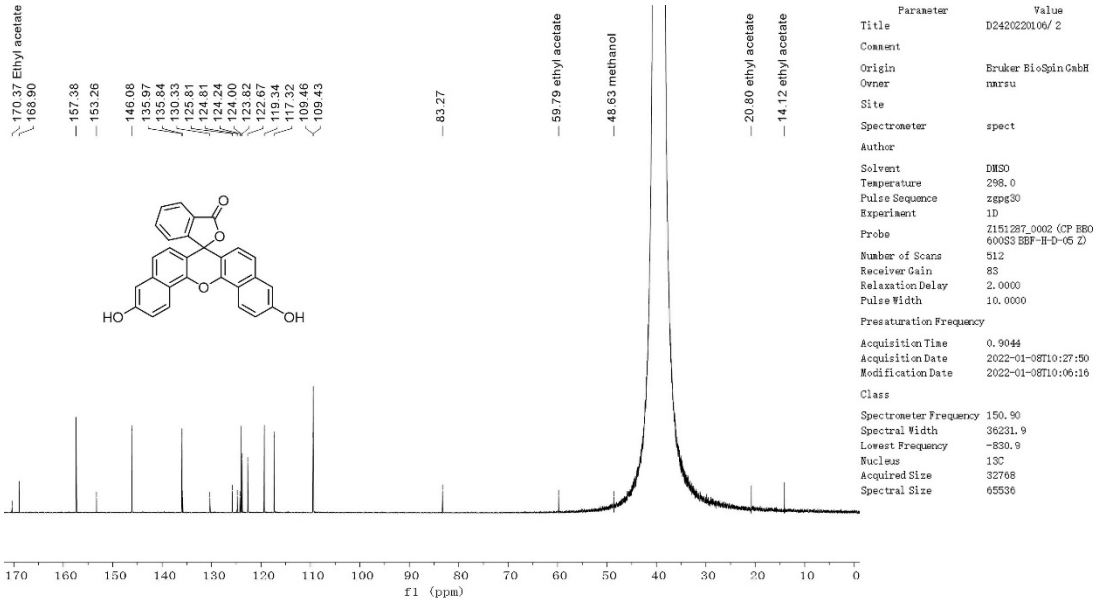

Figure S14. ^{13}C NMR spectrum of **NAF-OH**.

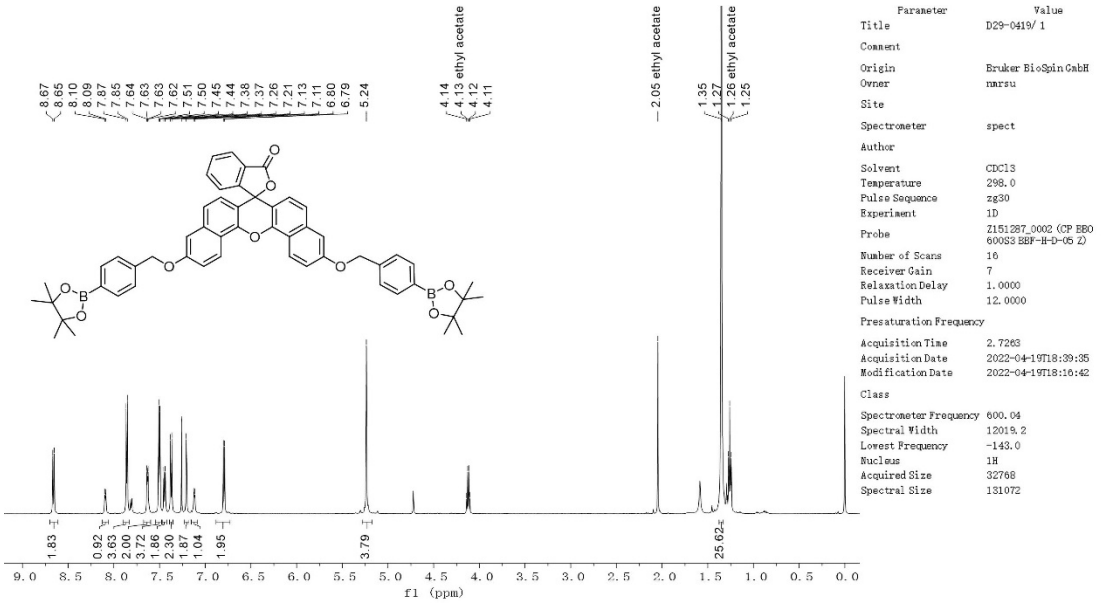

Figure S15. ^{1}H NMR spectrum of **NAF-BN**.

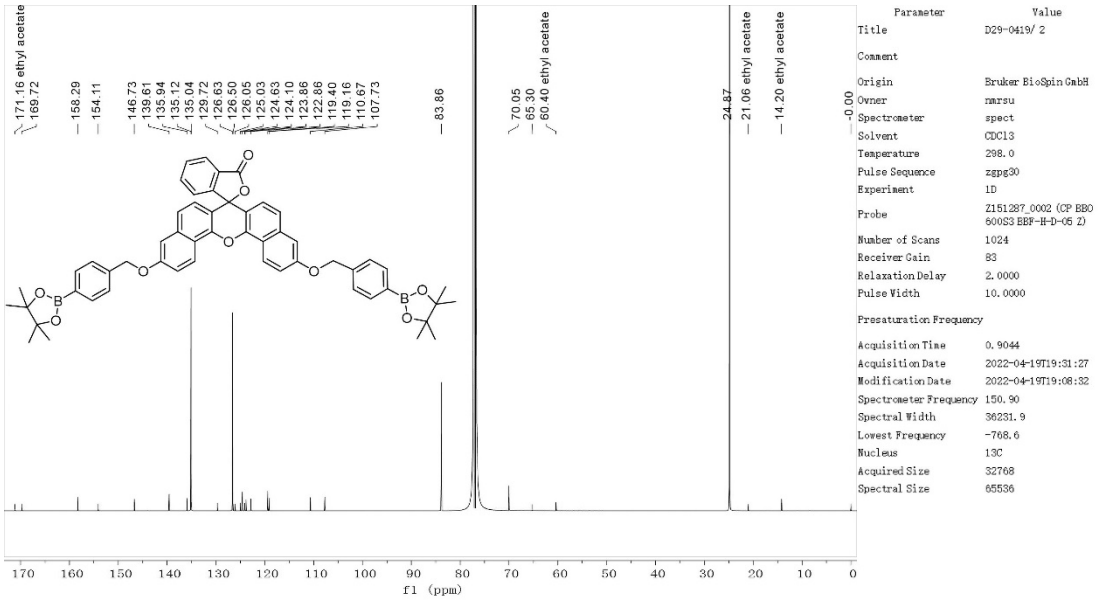

Figure S16. ^{13}C NMR spectrum of **NAF-BN**.

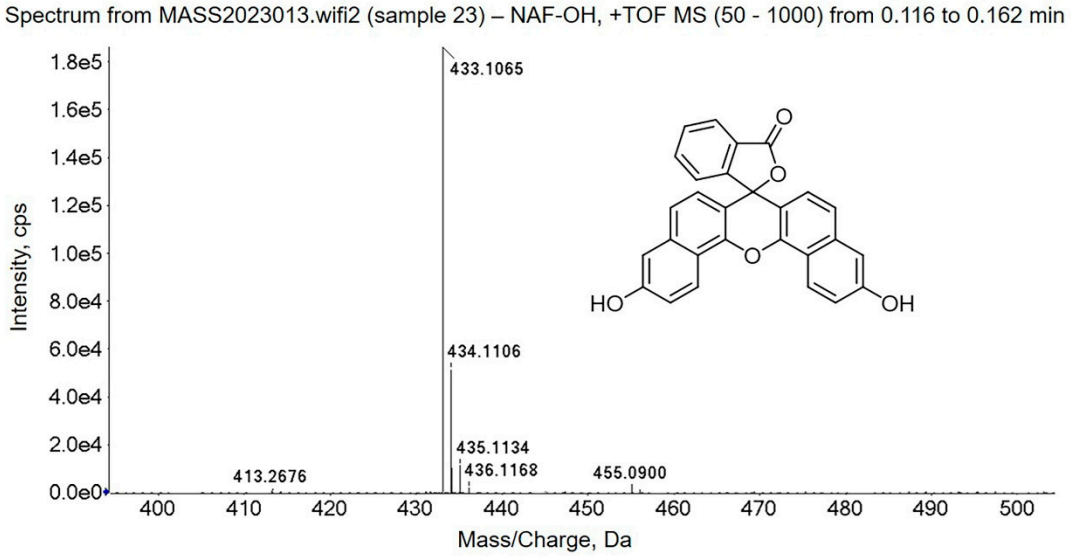

Figure S17. HRMS spectrum of **NAF-OH**.

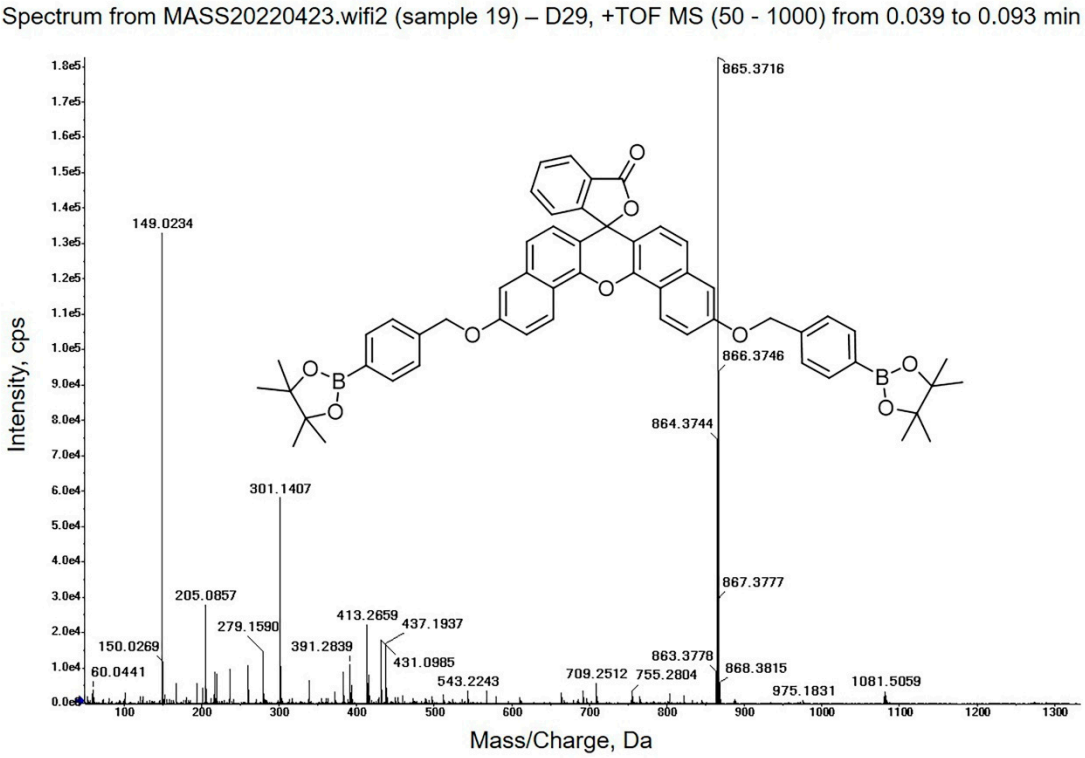

Figure S18. HRMS spectrum of **NAF-BN**.

References

1. Sun, Q.; Xu, J.; Ji, C.; Shaibani, M.S.S.; Li, Z.; Lim, K.; Zhang, C.; Li, L.; Liu, Z. Ultrafast Detection of Peroxynitrite in Parkinson's Disease Models Using a near-Infrared Fluorescent Probe. *Anal. Chem*. **2020**, *92*, 4038–4045. https://doi.org/10.1021/acs.analchem.9b05599.
2. Li, H.; Shi, W.; Li, X.; Hu, Y.; Fang, Y.; Ma, H. Ferroptosis Accompanied by •OH Generation and Cytoplasmic Viscosity Increase Revealed Via Dual-Functional Fluorescence Probe. *J Am Chem Soc* **2019**, *141*, 18301–18307. doi:10.1021/jacs.9b09722.
3. Massey, V.; Komai, H.; Palmer, G.; Elion, G.B. On the Mechanism of Inactivation of Xanthine Oxidase by Allopurinol and Other Pyrazolo[3,4-D]Pyrimidines. *J Biol Chem* **1970**, *245*, 2837–2844. doi:10.1016/s0021-9258(18)63065-0.
4. Suo, F.T.; Chen, X.W.; Fang, H.X.; Gong, Q.Y.; Yu, C.M.; Yang, N.D.; Li, S.; Wu, Q.; Li, L.; Huang, W. Hybrid Fluorophores-Based Fluorogenic Paper Device for Visually High-Throughput Detection of Cu^{2+} in Real Samples. *Dyes Pigm* **2019**, *170*, 107639. doi:10.1016/j.dyepig.2019.107639.